J Med Ultrasonics (2013) 40:91–98
DOI 10.1007/s10396-012-0400-9

ORIGINAL ARTICLE

Measurement of regional pulse wave velocity using very high frame rate ultrasound

Hideyuki Hasegawa · Kazue Hongo · Hiroshi Kanai

Received: 1 May 2012 / Accepted: 1 August 2012 / Published online: 10 October 2012

Abstract
Purpose Pulse wave velocity (PWV) is the propagation velocity of the pressure wave along the artery due to the heartbeat. The PWV becomes faster with progression of arteriosclerosis and, thus, can be used as a diagnostic index of arteriosclerosis. Measurement of PWV is known as a noninvasive approach for diagnosis of arteriosclerosis and is widely used in clinical situations. In the traditional PWV method, the average PWV is calculated between two points, the carotid and femoral arteries, at an interval of several tens of centimeters. However, PWV depends on part of the arterial tree, i.e., PWVs in the distal arteries are faster than those in the proximal arteries. Therefore, measurement of regional PWV is preferable.
Methods To evaluate regional PWV in the present study, the minute vibration velocity of the human carotid arterial wall was measured at intervals of 0.2 mm at 72 points in the arterial longitudinal direction by the *phased-tracking method* at a high temporal resolution of 3472 Hz, and PWV was estimated by applying the Hilbert transform to those waveforms.
Results In the present study, carotid arteries of three healthy subjects were measured in vivo. The PWVs in short segments of 14.4 mm in the arterial longitudinal direction were estimated to be 5.6, 6.4, and 6.7 m/s, which were in good agreement with those reported in the literature. Furthermore, for one of the subjects, a component was clearly found propagating from the periphery to the direction of the heart, i.e., a well known component reflected by the peripheral arteries. By using the proposed method, the propagation speed of the reflection component was also separately estimated to be −8.4 m/s. The higher magnitude of PWV for the reflection component was considered to be the difference in blood pressure at the arrivals of the forward and reflection components.
Conclusion Such a method would be useful for more sensitive evaluation of the change in elasticity due to progression of arteriosclerosis by measuring the regional PWV in a specific artery of interest (not the average PWV including other arteries).

Keywords Regional pulse wave velocity · Parallel beam forming · High frame rate

Introduction

The number of patients suffering from arteriosclerosis is rapidly increasing with the aging of society and dietary westernization. It is important to make an early diagnosis of arteriosclerosis to prevent serious diseases such as myocardial and cerebral infarction.

Recently, there are many methods for diagnosis of arteriosclerosis, such as angiography, intra-vascular ultrasound (IVUS), optical coherence tomography (OCT), computed tomography (CT), magnetic resonance imaging (MRI), and positron emission tomography (PET) [1–3]. These methods are invasive and/or not easily applicable. Therefore, they are unsuitable for repetitive diagnosis to monitor progression of arteriosclerosis. On the other hand, diagnosis with ultrasound is noninvasive, easy to use at bedside, and suitable for repetitive diagnosis.

Ultrasound B-mode imaging is widely used for the morphological diagnosis of the arterial wall, particularly for

H. Hasegawa · K. Hongo · H. Kanai
Graduate School of Biomedical Engineering, Tohoku University,
6-6-05 Aramaki-aza-Aoba, Aoba-ku, Sendai 980-8579, Japan

H. Hasegawa (✉) · H. Kanai
Graduate School of Engineering, Tohoku University,
6-6-05 Aramaki-aza-Aoba, Aoba-ku, Sendai 980-8579, Japan
e-mail: hasegawa@ecei.tohoku.ac.jp

measurement of intima-media thickness [4–6]. In addition, methods for evaluating the elasticity and viscosity of the arterial wall have recently been developed [7–13]. For diagnosis of early-stage arteriosclerosis, it is useful to evaluate the elastic property of the arterial wall because arterial-wall elasticity changes with progression of arteriosclerosis [14].

For noninvasive clinical evaluation of arterial elasticity, the pulse wave velocity (PWV) method was developed for diagnosis of arteriosclerosis nearly 100 years ago [15, 16]. This method measures the pulse wave, which is the pressure wave generated by the heartbeat, that propagates in the longitudinal direction of the artery. Since PWV c_{PWV} becomes faster with progression of arteriosclerosis, it is used as a diagnostic index of arteriosclerosis and is expressed by the Moens–Korteweg equation as follows [16]:

$$c_{\mathrm{PWV}} = \sqrt{\frac{E_\theta h}{\rho D}}, \tag{1}$$

where E_θ is the Young's modulus in the circumferential direction of the artery, h is the thickness of the arterial wall, ρ is the blood density, and D is the diameter of the artery. The assumptions underlying the Moens–Korteweg equation are that the artery has a thin wall and is filled with an incompressible inviscid liquid. Since PWV is traditionally measured between the carotid artery and femoral artery (cfPWV (carotid-femoral PWV) method) [17, 18] it is not suitable for early diagnosis of arteriosclerosis because lesions of early-stage arteriosclerosis are several millimeters in size. In addition, PWV depends on a part of the arterial tree, i.e., PWV in the distal arteries is faster than that in the proximal arteries. Thus, measurement of regional PWV would be useful for diagnosis of early-stage arteriosclerosis.

We previously studied regional PWVs by measuring small vibration velocities of the arterial wall at two points along the arterial longitudinal direction [19]. To estimate regional PWV more accurately, in the present study, vibration velocities at multiple points in a region of about 14 mm along the arterial longitudinal direction were measured at a high temporal resolution of 3472 Hz. Vibration velocities of the arterial wall have frequency components mostly up to 30 Hz. However, a high temporal resolution is desirable to estimate a small time delay between vibration velocities due to pulse wave propagation, i.e., the pulse wave propagates a region of about 14 mm in 2.8 ms when PWV is 5 m/s.

Materials and methods

Measurement of small vibration velocity for the carotid arterial wall

In the present study, as illustrated in Figs. 1 and 2, minute vibration velocities of the human carotid arterial wall were measured by the *phased-tracking method* [20] at 72 points in the arterial longitudinal direction with intervals of 0.2 mm (total length of 14.4 mm) at a high temporal resolution of 3472 Hz. Modified ultrasonic diagnostic equipment (Aloka, α-10) was used to acquire ultrasonic RF echoes received by each transducer element [21, 22]. The center frequency and fractional bandwidth of an emitted ultrasound pulse were 8 MHz and 61 %, respectively. The received RF echo was sampled at 40 MHz with 16-bit resolution. The method for high frame rate imaging developed by our group [21] was used to obtain beamformed ultrasonic RF echoes at 72 beam positions at a very high frame rate of 3472 Hz.

Typical PWV is several m/s and passes through a small region of 14.4 mm in a very short period of a few milliseconds. In such a situation, a small random error in estimation of the time delay between velocity waveforms would lead to a significant error in estimation of PWV when PWV is estimated using velocities measured at only two points along the arterial longitudinal direction. Therefore, in the present study, vibration velocities were measured at multiple points to reduce random errors, such as electrical noise and arterial motion estimation error due to random interference of echoes from scatterers in the arterial wall [13].

In the *phased-tracking method*, ultrasonic pulses at angular frequency $\omega_0 = 2\pi f_0$ were transmitted from an ultrasonic transducer placed on the skin surface at a time interval of $\Delta T = 1/f_{\mathrm{FR}}$ (f_{FR}: frame rate) at each ultrasonic beam position. The instantaneous distance between the moving arterial wall and the ultrasonic transducer is denoted by $z(t) = c_0\tau_{\mathrm{u}}(t)/2$, where c_0 is the velocity of ultrasound, and $\tau_{\mathrm{u}}(t)$ is the time delay required for two-way transmission between the ultrasonic transducer and the arterial wall. The phase $\theta(z;t)$ of the quadrature demodulated signal of the received ultrasonic echo is given by $\theta(z;t) = \omega_0\tau_{\mathrm{u}}(t) = 2\omega_0 z(t)/c_0$. The phase difference $\Delta\theta(z;t)$ between time t and $(t + \Delta T)$ is given by

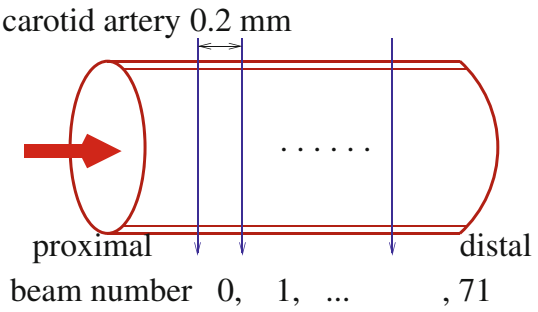

Fig. 1 Illustration of measurement of minute vibration velocity waveforms of the human carotid arterial wall at 72 points at intervals of 0.2 mm

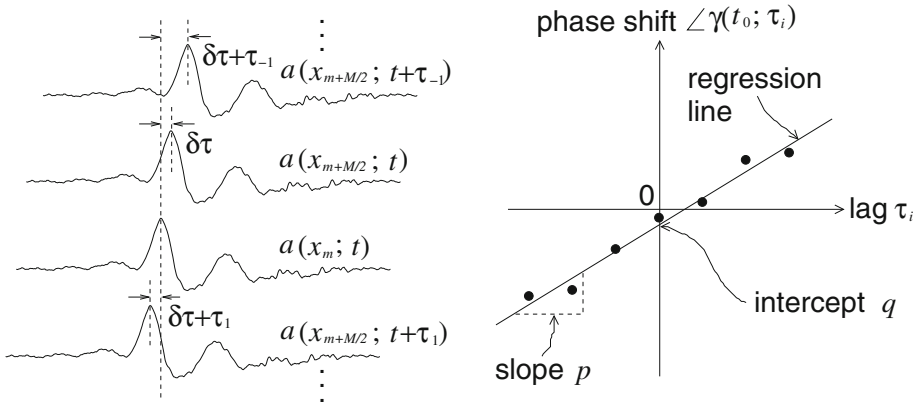

Fig. 2 Illustration of the method for estimation of time delay between acceleration waveforms $a(x_m; t)$ and $\{a(x_{m+M/2}; t + \tau_i)\}$ using their analytic signals

$$\Delta\theta(z;t) = \theta(z;t+\Delta T) - \theta(z;t) = \frac{2\omega_0 \Delta z(t)}{c_0}, \tag{2}$$

where $\Delta z(t) = z(t+\Delta T) - z(t)$ is the displacement of an object during the period ΔT. By dividing the displacement Δz by the period ΔT, the average velocity, denoted by $v(t + \Delta T/2)$, of the object during the period ΔT is given by the phase difference $\Delta\theta(z;t)$ between echoes as follows:

$$v\left(t+\frac{\Delta T}{2}\right) = \frac{\Delta z(t)}{\Delta T} = -\frac{c_0}{2\Delta T}\frac{\Delta\theta(z;t)}{\omega_0}, \tag{3}$$

In the present study, parallel beam forming (PBF) [21] was applied to realize a high frame rate of 3472 Hz. The minute vibration velocity waveforms were measured at 72 points on the human carotid artery wall at intervals of 0.2 mm.

Estimation of PWV by complex correlation approach

In the present study, the acceleration waveforms $\{a(x_m; t)\}$ were obtained by applying time differentiation to the vibration velocity waveforms $\{v(x_m; t)\}$, where x_m is the mth ultrasonic beam position, to enhance high frequency components contained in the measured velocity waveforms because the use of high frequency components improves the time resolution in estimation of time delays among the vibration waveforms due to the propagation of the pulse wave. To estimate PWV, the phase $\phi(x_m; t_0)$ of acceleration waveform $a(x_m; t_0)$ at a time of interest t_0 (=frame) measured at the mth ultrasonic beam position x_m is obtained by applying the Hilbert transform to the acceleration waveforms $\{a(x_m; t)\}$. The Hilbert transform was applied to the acceleration waveforms during just an entire cardiac cycle. The phase $\phi(x_m; t)$ is determined from the complex analytic signal $g(x_m; t)$ of $a(x_m; t)$.

To determine the PWV from the phases of the multiple analytic signals, a method based on the complex cross correlation function was developed in the present study. The complex cross correlation function $\gamma(t_0, \tau_i)$ at t_0 at lag $\tau_i = i \cdot \Delta T$, where $i = -N_l, -N_l + 1, \ldots, -1, 0, 1, \ldots, N_l - 1, N_l$ (N_l denotes the number of lags used in estimation of PWV), is defined as follows:

$$\widehat{\gamma}(t_0, \tau_i) = \sum_{m=0}^{M/2} \sum_{i=-N_c}^{N_c} g^*(x_m; t_0) \cdot g(x_{m+M/2}; t_0 + \tau_i), \tag{4}$$

where $\tau_i = i \cdot \Delta T$, M is the number of ultrasonic beam positions, and N_c determines the number of frames used for calculation of the complex correlation function.

By denoting the original time delay of $g(x_{m+M/2}; t_0)$ from $g(x_m; t_0)$ due to the propagation of the pulse wave in the length of $\delta x \cdot M/2$ (δx: lateral spacing of ultrasonic beams) by $\delta\tau$ and denoting the dominant frequency of $\{g(x_m; t_0)\}$ at t_0 by f_a, $\delta\tau$ is expressed as follows:

$$\delta\tau = -\frac{\angle\gamma(t_0, 0)}{2\pi f_a}. \tag{5}$$

For other lag τ_i, the model $\angle\widehat{\gamma}(t_0, \tau_i)$ of the phase of $\gamma(t_0, \tau_i)$ is expressed as follows:

$$\begin{aligned} \angle\widehat{\gamma}(t_0, \tau_i) &= 2\pi f_a(\tau_i - \delta\tau) \\ &= 2\pi f_a \cdot (i \cdot \Delta T) - 2\pi f_a \delta\tau\,. \\ &\equiv p \cdot i + q. \end{aligned} \tag{6}$$

To estimate the dominant frequency f_a and time delay $\delta\tau$ due to propagation of the pulse wave, the coefficients p and q are determined by fitting a linear function defined by Eq. (6) to measured $\{\angle\gamma(t_0, \tau_i)\}$ using the least squares method as follows: the difference $\alpha(t_0)$ between the angle of the measured complex correlation function $\angle\gamma(t_0, \tau_i)$ and the model $\angle\widehat{\gamma}(t_0, \tau_i)$ is expressed as follows:

$$\alpha(t_0) = \sum_{i=-N_l}^{N_l} |\angle\gamma(t_0, \tau_i) - (p \cdot i + q)|^2. \tag{7}$$

To determine the coefficients $\widehat{p}$ and $\widehat{q}$, which minimize $\alpha(t_0)$, partially differentiated $\alpha(t_0)$ with respect to p and q are set to zero. By solving the resultant simultaneous equations, the coefficients p and q are determined as follows:

$$\widehat{p} = \frac{(2N_c+1)\left\{\sum_{i=-N_c}^{N_c} i \cdot \angle\gamma(t_0,\tau_i)\right\} - \left(\sum_{i=-N_c}^{N_c} i\right)\left\{\sum_{i=-N_c}^{N_c} \angle\gamma(t_0,\tau_i)\right\}}{(2N_c+1)\left(\sum_{i=-N_c}^{N_c} i^2\right) - \left(\sum_{i=-N_c}^{N_c} i\right)^2}. \quad (8)$$

$$\widehat{q} = \frac{\widehat{p}\sum_{i=-N_c}^{N_c} i - \sum_{i=-N_c}^{N_c} \angle\gamma(t_0,\tau_i)}{(2N_c+1)}. \quad (9)$$

Based on Eq. (6), the dominant frequency f_a is determined using the estimated coefficient $\widehat{p}$ as follows:

$$\widehat{f_a} = \frac{\widehat{p}}{2\pi\Delta T}. \quad (10)$$

Finally, PWV $c_{PWV}(t_0)$ is estimated based on Eq. (6) using the estimated dominant frequency $\widehat{f_a}$ and coefficient $\widehat{q}$ as follows:

$$c_{PWV}(t_0) = \frac{\frac{M}{2}\cdot\delta x}{\widehat{\delta\tau}} = -\frac{\pi\widehat{f_a}\cdot M\cdot\delta x}{\widehat{q}}. \quad (11)$$

In Eq. (4), the complex correlation function between analytic signals $\{g(x_m;\ t_0)\}$ and $\{g(x_{m+M/2};\ t_0)\}$ was used because the distance between each pair of the analytic signals should be as large as possible to increase the time delay between the analytic signals and also all the M analytic signals can be used to reduce random errors.

Results

Figure 3a–c shows the B-mode images of 24-(subject A), 23-(subject B), and 38-(subject C) year-old males, respectively. Figures 4, 5, and 6 show in vivo experimental results of subjects A, B, and C, respectively. The short segments of their common carotid arteries of 14.4 mm ((72 beam positions) × (0.2 beam spacing)) were measured. In each of Figs. 4, 5, and 6, electrocardiogram (ECG) (a); the displacement waveform (b), which is obtained by integrating the vibration velocity in (c) with respect to time; vibration velocity measured at the 0th beam position (the 0th beam was nearest to the heart) (c); and the acceleration waveform (d), which is obtained by temporal differentiation of the vibration velocity in (c), are shown. Velocities at the media-adventitia boundaries of the posterior walls were measured as the vibration velocities of the arterial walls.

The vibration of the arterial wall is generated by the ejection of blood from the left ventricle of the heart, and expansion of the artery corresponds to the acceleration waveform around 0.1 s. For example, the enlarged view of the acceleration waveforms of subject A measured at the 0th (proximal) and 71st (distal) beams during a period 0–0.3 s is shown in Fig. 7. As can be seen in Fig. 7, it is recognized that the positive peak around 0.07 s at the 0th beam precedes that of the 71st beam very slightly. In the present study, the large positive peak around $t = 0.1$ s (t_0 for estimation of PWV is shown by the vertical dashed line in Fig. 4), which was caused by ejection of blood from the left ventricle, was analyzed for estimation of PWV.

To estimate PWVs, the Hilbert transform was applied to the acceleration waveforms. The complex cross correlation function defined in Eq. (4) was obtained by setting t_0 to be the time of the peak in the acceleration waveform measured at the 0th beam position around 0.1 s. The assigned t_0 is shown by the vertical dashed lines in Figs. 4, 5, and 6. The length of the correlation window was set at 10 ms (corresponding to $N_c = 17$), which roughly corresponded to the width of the peak in the acceleration waveform. Plots in Fig. 8 show the measured phase $\angle\gamma(t_0,\tau_i)$ of the complex correlation function plotted as a function of the lag τ_i. The PWV was estimated from the slope $\widehat{p}$ and intercept $\widehat{q}$ of the regression line (shown by the dashed line in Fig. 8) based on Eq. (11). By applying the same procedure to the acceleration waveforms of subjects B and C, regional PWVs of subjects A, B, and C were estimated to be 5.6, 6.4, and 6.7 m/s, respectively. The estimated pulse wave velocities were similar to those reported in the literature [23–25].

By observing the acceleration waveform of subject A (shown in Fig. 4d), there is a small but distinct peak around the time of 0.2 s. In the literature, such a peak detected in the acceleration waveform is reported to be a pulse wave component reflected in the distal position of the arterial tree [26–28]. As can be seen in Fig. 7, the acceleration waveform at the 71st beam (nearer to the head) precedes that at the 0th beam very slightly. The PWV for this component was estimated by setting t_0 to the time of the peak in the acceleration waveform measured at the 0th beam position around 0.2 s (t_0 for this reflection component and is shown by the vertical dashed line in Fig. 4). The estimated PWV for the reflection component was −8.4 m/s, where the negative velocity means the propagation from the periphery to the heart. As described above, the regional PWV of the reflection component could also be estimated separately using the proposed method.

Furthermore, for evaluation of the reproducibility of measurements using the proposed method, five additional

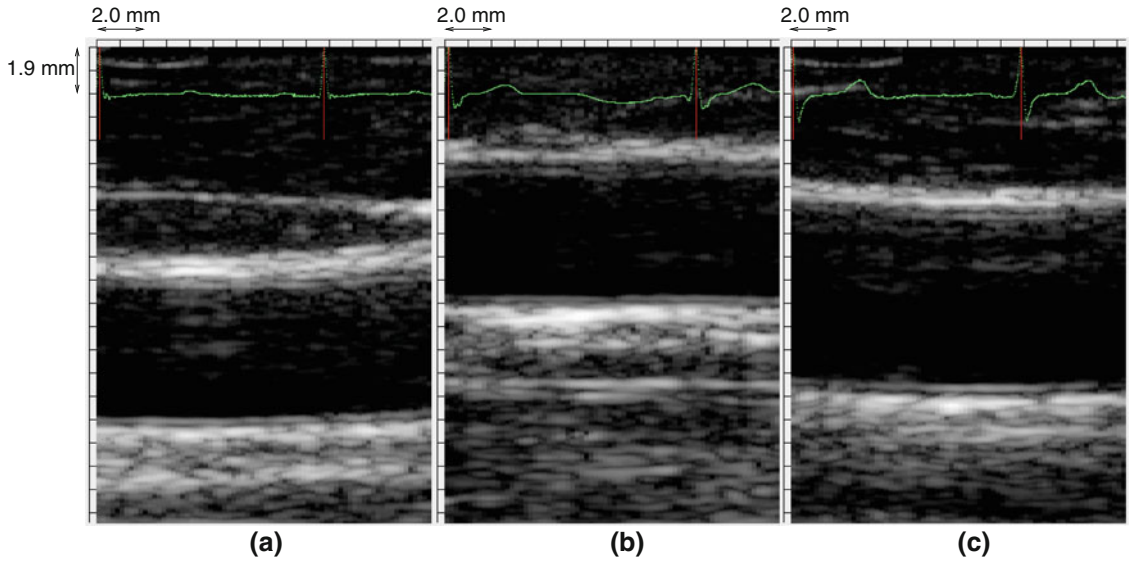

Fig. 3 B-mode images of carotid arteries of 23-(subject A), 24-(subject B), and 38-(subject C) year-old healthy males

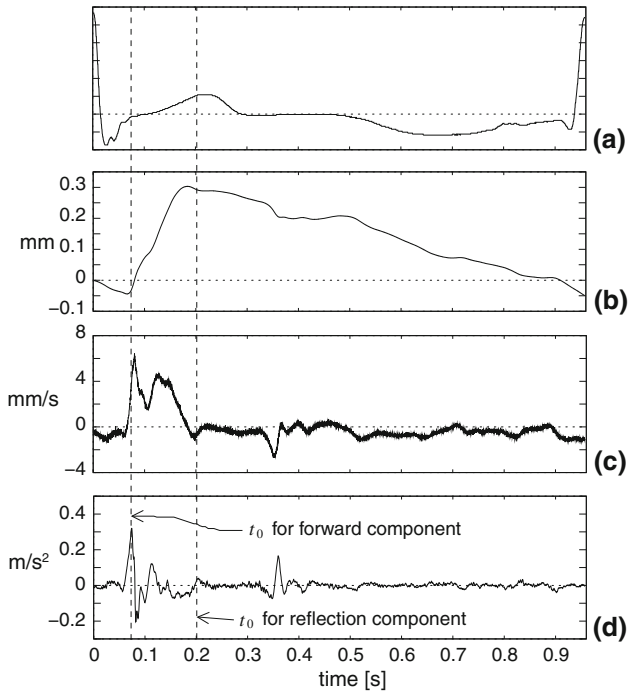

Fig. 4 In vivo experimental results of subject A. **a** Electrocardiogram, **b** displacement, **c** velocity $v(x_m; t)$, and **d** acceleration $a(x_m; t)$ of the posterior wall measured at the 0th ultrasonic beam

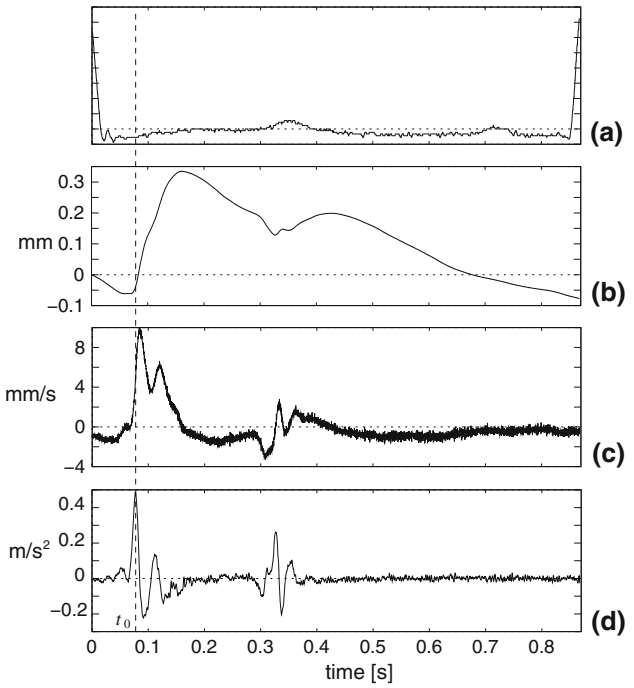

Fig. 5 In vivo experimental results of subject B. **a** Electrocardiogram, **b** displacement, **c** velocity $v(x_m; t)$, and **d** acceleration $a(x_m; t)$ of the posterior wall measured at the 0th ultrasonic beam

measurements were performed with respect to subject C on the same day. Figure 9a shows acceleration waveforms in the 0th scan lines for the five measurements. Using the phase $\angle\gamma(t_0; \tau_i)$ of the complex correlation function shown in Fig. 9b, the regional pulse wave velocities were estimated. The mean and standard deviation for the five measurements were 7.0 and 0.72 m/s (10.4 % of the mean value), respectively.

Discussion

For one of the subjects in the present study, a pulse wave component, which was considered to be reflected by the distal arterial tree, was found. By applying the Hilbert transform and the proposed complex cross correlation technique to the acceleration waveforms obtained by differentiating the measured velocity waveforms, the forward

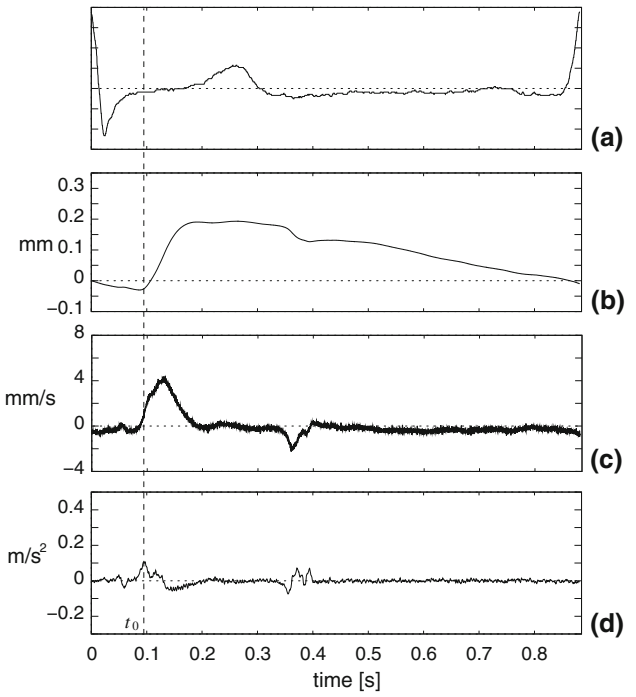

Fig. 6 In vivo experimental results of subject C. **a** Electrocardiogram, **b** displacement, **c** velocity $v(x_m; t)$, and **d** acceleration $a(x_m; t)$ of the posterior wall measured at the 0th ultrasonic beam

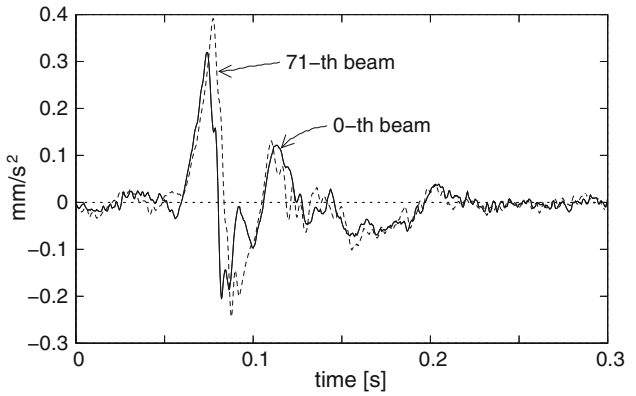

Fig. 7 Enlarged view of the acceleration waveforms $\{a(x_m; t)\}$ of subject A during 0–0.3 s measured at the 0th (*solid line*) and 71th (*dashed line*) ultrasonic beams

and reflection components were separately analyzed. The estimated propagation speed of the forward component was lower (5.6 m/s) than that (8.4 m/s in the opposite direction) of the reflection component. One of the reasons for this difference was considered to be the difference between blood pressures at the arrival times of the forward and reflection components in the carotid artery.

It was reported that the arterial wall distension waveform can be assumed to be the waveform of blood pressure [29–31]. Figure 4b shows the displacement of the posterior arterial wall obtained by integrating the measured velocity

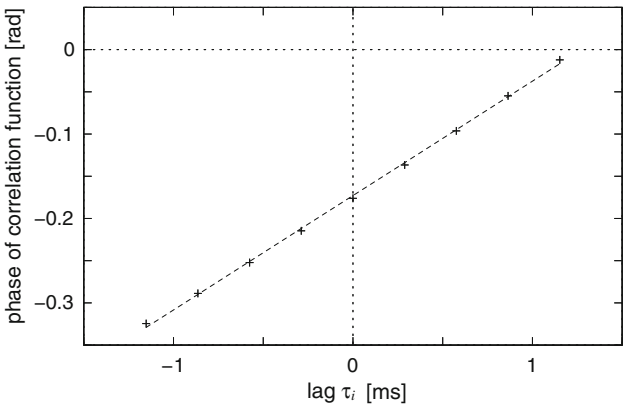

Fig. 8 Phase of complex correlation function $\angle\gamma(t_0, \tau_i)$ plotted as a function of lag τ_i. *Plots* and the *dashed line* show measured phases and the regression line

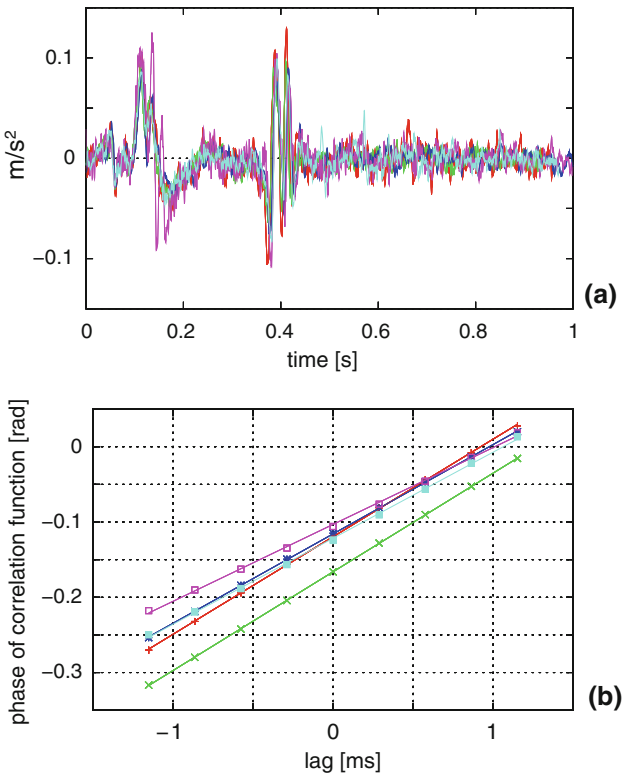

Fig. 9 **a** Acceleration waveforms in the 0th scan lines measured for the five additional measurements with respect to subject C. **b** Phases of complex correlation functions $\{\angle\gamma(t_0, \tau_i)\}$ plotted as a function of lag τ_i. *Plots* and *lines* show measured phases and the regression lines

waveform with respect to time. At the time (around 0.1 s) of the peak of the forward component in the acceleration waveform shown in Fig. 4d, the magnitude of the displacement is nearly zero. This fact suggests that blood pressure at the arrival of the forward component corresponds to the diastolic blood pressure. On the other hand, the displacement at the time of the arrival of the reflection component is nearly maximum, which suggests that blood

pressure at the time of arrival of the reflection component is nearly the systolic blood pressure. It is also reported that the stress–strain relationship of the arterial wall is nonlinear [32–35], and the elastic modulus of the arterial wall at higher blood pressure is larger than that at lower blood pressure. Therefore, the PWV of the reflection component (presumably at higher blood pressure) was considered to be larger than that at the forward component.

In the present study, the propagation of pulse waves in a local region in the carotid artery was analyzed in detail by measuring vibration velocities of the arterial wall at a very high temporal resolution of 3472 Hz. To measure the regional PWV in an arterial longitudinal segment of about 15 mm, a small time delay of a few milliseconds between vibration waveforms of the arterial wall needs to be estimated. For this purpose, in the present study, acceleration waveforms, which contain higher frequency components compared with displacement waveforms, were measured at a high temporal resolution, and a method for estimation of a small time delay using the phase of the acceleration waveform was developed.

Figures 10b–d show the displacement, velocity, and acceleration waveforms sampled at a frame rate of 35 Hz (waveforms in Fig. 4 were down sampled), which is a typical frame rate of conventional ultrasonic diagnostic equipment. As shown in Fig. 10, it is difficult to measure the velocity and acceleration waveforms at a temporal resolution of 35 Hz. Using the displacement waveform shown in Fig. 10d, which was sampled at 35 Hz, the pulse wave velocity was also estimated by the proposed method described in "Estimation of PWV by a complex correlation approach". The estimated PWV was −37.2 m/s, which was significantly different from that reported in the literature. Therefore, it is necessary to measure the vibration waveform at a high temporal resolution.

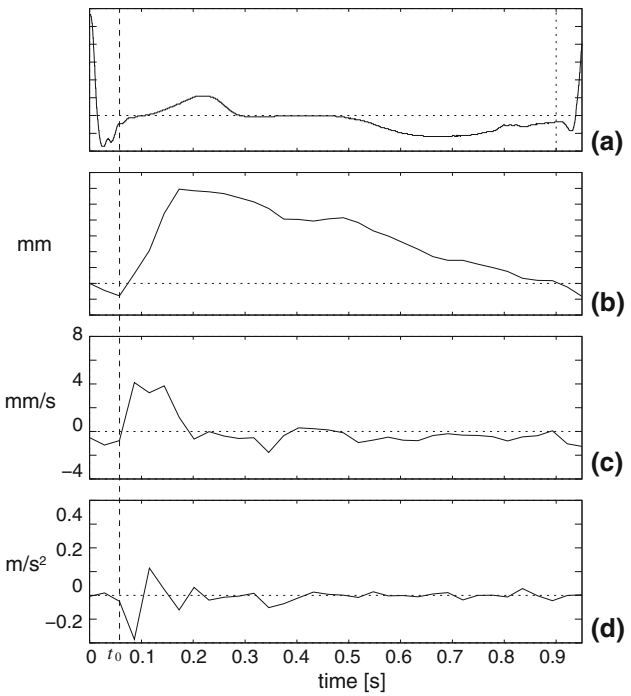

Fig. 10 Vibration waveforms of subject A (waveforms in Fig. 4 are down sampled at 35 Hz). **a** Electrocardiogram, **b** displacement, **c** velocity $v(x_m; t)$, and **d** acceleration $a(x_m; t)$ of the posterior wall measured at the 0th ultrasonic beam

As described above, in the present study, regional pulse wave velocities were noninvasively measured in vivo by the proposed method and compared with those reported in the literature. In future studies, it will be necessary to evaluate the accuracy of estimation of regional PWV using the proposed method by basic experiments using phantoms. In addition, the conditions of the spacing and number of scan lines and frame rate, etc., required for measurement of regional PWV also need to be investigated by phantom experiments. However, the results obtained in the present study show the possibility of the proposed method for measurement of regional PWV, and such a method would be useful for diagnosis of arteriosclerosis.

Conclusion

For detailed analyses of pulse wave propagation in a local region of 14.4 mm in the carotid artery, in the present study, small vibrations on the arterial wall were measured with ultrasound at a very high frame rate of 3472 Hz. By applying the Hilbert transform to the acceleration waveforms of the arterial wall, which were obtained by differentiating the measured vibration velocity waveforms, pulse wave velocities of three healthy subjects were estimated using the proposed complex cross correlation approach. Furthermore, in one of the subjects, there was a component propagating from the heart to the periphery and from the periphery to the heart. Even in such a case, pulse wave velocities for these forward and reflection components were separately estimated, and the magnitudes of the estimated pulse wave velocities were similar to those reported in the literature. Such a method for measurement of regional PWV would be useful for more sensitive evaluation of the change in elasticity due to progression of arteriosclerosis.

Conflict of interest None.

References

1. Ibanez B, Badimon JJ, Garcia MJ. Diagnosis of arteriosclerosis by imaging. Am J Med. 2009;122:S15–25.
2. Sakalihasan N, Limet R, Defawe OD. Abdominal aortic aneurysm. Lancet. 2005;365:1577–89.

3. Vorp DA. Biomechanics of abdominal aortic aneurysm. J Biomech. 2007;40:1887–902.
4. Wendelhag I, Wiklund O, Wikstrand J. On quantifying plaque size and intima-media thickness in carotid and femoral arteries: comments on results from a prospective ultrasound study in patients with familial hypercholesterolemia. Arterioscler Thromb Vasc Biol. 1996;16:843–50.
5. Liang Q, Wendelhag I, Wilstrand J, Gustavsson T. A multiscale dynamic programming procedure for boundary detection in ultrasonic artery images. IEEE Trans Med Imaging. 2000;19:127–42.
6. Klingensmith JD, Shekhar R, Vince DG. Evaluation of three-dimensional segmentation algorithms for the identification of luminal and media-adventitial borders in intravascular ultrasound images. IEEE Trans Med Imaging. 2000;19:996–1011.
7. Meinders JM, Brands PJ, Willigers JM, Kornet L, Hoeks APG. Assessment of the spatial homogeneity of artery dimension parameters with high frame rate 2-D B-mode. Ultrasound Med Biol. 2001;27:785–94.
8. Kanai H, Hasegawa H, Ichiki M, Tezuka F, Koiwa Y. Elasticity imaging of atheroma with transcutaneous ultrasound: preliminary study. Circulation. 2003;107:3018–21.
9. Maurice J, Ohayon J, Frétigny Y, Bertrand M, Soulez G, Cloutier G. Noninvasive vascular elastography: theoretical framework. IEEE Trans Med Imaging. 2004;23:164–80.
10. Tsuzuki K, Hasegawa H, Ichiki M, Tezuka f, Kanai H. Optimal region-of-interest settings for tissue characterization based on ultrasonic elasticity imaging. Ultrasound Med Biol. 2008;34:573–85.
11. Ikeshita K, Hasegawa H, Kanai H. Flow-mediated change in viscoelastic property of radial arterial wall measured by 22-MHz ultrasound. Jpn J Appl Phys. 2009;48:07GJ10-1–5.
12. Ikeshita K, Hasegawa H, Kanai H. Noninvasive measurement of transient change in viscoelasticity due to flow-mediated dilation using automated detection of arterial wall boundaries. Jpn J Appl Phys. 2011;50:07HF08-1–7.
13. Hasegawa H, Kanai H. Reduction of influence of variation in center frequencies of RF echoes on estimation of artery-wall strain. IEEE Trans Ultrason Ferroelectr Freq Control. 2008;55:1921–34.
14. Tokita A, Ishigaki Y, Okimoto H, Hasegawa H, Koiwa Y, Kato M, Ishihara H, Hinokio Y, Katagiri H, Kanai H, Oka Y. Carotid arterial elasticity is a sensitive atherosclerosis value reflecting visceral fat accumulation in obese subjects. Atherosclerosis 2009;206:168–72.
15. Bramwell JC, Hill AV. The velocity of the pulse wave in man. Biol Sci. 1922;93:298–306.
16. Halloc P. Arterial elasticity in man in relation to age as evaluated by pulse wave velocity method. Arch Int Med. 1934;54:770–98.
17. Laurent S, Cockcroft J, Bortel L, Boutouyrie P, Giannattasio C, Hayoz D, Pannier B, Vlachopoilos C, Wilkinson I, Struijker-Boudier H. Expert consensus document on arterial stiffness: methodological issues and clinical applications. Eur Heart J. 2006;27:2588–605.
18. Imura T, Yamamoto K, Kanamori K, Mikami T, Yasuda H. Noninvasive ultrasonic measurement of the elastic properties of the human abdominal aorta. Cardiovasc Res. 1986;20:208–14.
19. Kanai H, Kawabe K, Takano M, Murata R, Chubachi N, Koiwa Y. New method for evaluating local pulse wave velocity by measuring vibrations on arterial wall. Electron Lett. 1994;30:534–6.
20. Kanai H, Sato M, Koiwa Y, Chubachi N. Transcutaneous measurement and spectrum analysis of heart wall vibrations. IEEE Trans Ultrason Ferroelectr Freq Control. 1996;43:791–810.
21. Hasegawa H, Kanai H. Simultaneous imaging of artery-wall strain and blood flow by high frame rate acquisition of RF signals. IEEE Trans UFFC. 2008;55:2626–39.
22. Hasegawa H, Kanai H. High-frame-rate echocardiography using diverging transmit beams and parallel receive beamforming. J Med Ultrason. 2011;38:129–40.
23. Wilkinson IB, Fuchs SA, Jansen IM, Spratt JC, Murray GD, Cockcroft JR, Webb DJ. Reproducibility of pulse wave velocity and augmentation index measured by pulse wave analysis. J Hypertens. 1998;16:2079–84.
24. Rogers WJ, Hu YL, Coast D, Vido DA, Kramer CM, Pyerits RE, Reichek N. Age-associated changes in regional aortic pulse wave velocity. J Am Coll Cardiol. 2001;38:1123–9.
25. Nürnberger J, Saez AO, Dammer S, Mitchell A, Wenzel RR, Philipp T, Schäfers RF. Left ventricular ejection time: a potential determinant of pulse wave velocity in young, healthy males. J Hypertens. 2003;21:2125–32.
26. Iketani T, Iketani Y, Takazawa K, Yamashina A. The influence of the peripheral reflection wave on left ventricular hypertrophy in patients with essential hypertension. Hypertens Res. 2000;23:451–8.
27. Hayashi T, Nakayama Y, Tsumura K, Yoshimaru K, Ueda H. Reflection in the arterial system and the risk of coronary heart disease. Am J Hypertens. 2002;15:405–9.
28. London GM, Blacher J, Pannier B, Guérin AP, Marchais SJ, Safar ME. Arterial wave reflections and survival in end-stage renal failure. Hypertension. 2001;38:434–8.
29. Barnett GO, Mallos AJ, Shapiro A. Relationship of aortic pressure and diameter in the dog. J Appl Physiol. 1961;16:545–8.
30. Patel DJ, de Fretias FM, Greenfield JC Jr, Fly DL. Relationship of radius to pressure along the aorta in living dogs. J Appl Physiol. 1963;18:1111–7.
31. Sugawara M, Furuhata H, Kikkawa S, et al. Development of a non-invasive method of measuring blood pressure wave. Jpn J Med Electron Biol Eng. 1983;21S:429.
32. Newman DL, Gosling RG, Bowden NLR. Changes in aortic distensibility and area ratio with the development of atherosclerosis. Atherosclerosis. 1971;14:231–40.
33. Hudetz AG, Mark G, Kovach AGB, et al. Biomechanical properties of normal and fibrosclerotic human cerebral arteries. Atherosclerosis. 1981;39:353–65.
34. Young JT, Vaishnav RS, Patel DJ. Nonlinear elastic properties of canine arterial segments. J Biomech. 1977;10:549–59.
35. Guinea GV, Atienza JM, Elices M, Aragoncillo P, Hayashi K. Thermomechanical behavior of human carotid arteries in the passive state. Am J Physiol Heart Circ Physiol. 2005;288:H2940–5.